Perfluoro - polyether Microemulsions

Progress in Colloid & Polymer Science Progr Colloid Polym Sci 79:218–225 (1989)

Perfluoropolyether microemulsions

A. Chittofrati, D. Lenti, A. Sanguineti, M. Visca, C. M. C. Gambi[1]), D. Senatra[1]), and Z. Zhou[2])

Montefluos Spa, Colloid Laboratory, Spinetta Marengo, Italy
[1]) University of Florence, Department of Physics, Florence, Italy
[2]) On leave from Hubei University, People's Republic of China

Abstract: In the present paper a systematic investigation is presented of the phase behavior of perfluoropolyether (PFPE) surfactant, PFPE oil, water and isopropyl alcohol mixtures. Monophasic regions of isotropic, transparent, and fluid samples are identified in the thermal range 20° ÷ 60 °C. Preliminary data by light-scattering investigation support the hypothesis of the presence of O/W and W/O structural aggregates.

Key words: Perfluoropolyether (PFPE) polymers, PFPE microemulsions, phase diagrams on PFPE mixtures, light scattering on PFPE mixtures, DSC analysis on a PFPE surfactant.

Introduction

The aim of this work is to understand whether microemulsion's formation can take place by mixing perfluoropolyether (PFPE) surfactant, PFPE oil and water in both the presence and the absence of a short-chain hydrocarbon alcohol. The perfluoropolyethers (PFPE) used are fluorinated polymers produced by Montefluos (Milan, Italy) of general structure:

$$CF_3-[(O-CF_2-\underset{\displaystyle CF_3}{\underset{|}{CF}})_n-(O-CF_2)_m]-O- \qquad n/m = 20 \div 40$$

The properties of PFPE polymers, both oil and surfactant, and of their mixtures with water and alcohol have been reported in [1]. PFPE polymers have the main properties of fluorocarbons (thermal, chemical, and biological inertness, high permeability to gases, low compatibility with aqueous and hydrocarbon-based systems). The rigidity of the fluorocarbon chain (due to the bulky fluorine atoms) which allows fluorocarbons to be liquid only at very low molecular weights, is reduced in PFPE polymers by the etheral bridges of the polymer chains (C–O–C). The liquid state in PFPE is allowed even at molecular weights as high as 10,000 or more; the thermal range of the liquid state is also increased.

As fluorocarbon microemulsions have been prepared in the presence of fluorinated surfactants, for example as blood substitutes [2, 3], PFPE microemulsions, if they exist, could be prepared in wider molecular weight and temperature ranges.

Because the knowledge of the phase diagram is a fundamental basis to understand surfactant systems, this paper mainly focuses on the phase diagram investigation which has been performed on the binary, ternary and quaternary mixtures of PFPE surfactant, PFPE oil, water and isopropyl alcohol, in the thermal range 20° ÷ 60 °C; isopropyl alcohol has been chosen for its ability to sharply increase the surfactant solubility. The phase transition temperatures of the surfactant have been evidenced by differential scanning calorimetry in parallel with the visual observation of the surfactant properties in the range 20° ÷ 80 °C. Some surface tension and interfacial tension measurements as well as structural investigation by quasi-elastic light scattering and light intensity measurements have also been carried out.

Experimental

Materials

PFPE polymers are prepared industrially by U.V. photoinitiated oxidation of perfluoropropene at temperatures in the range −40° ÷

– 80 °C [4]. As an intermediate of the production process, functional products are obtained, characterized by a single carboxyl end group. The products are polydispersed; practically monodispersed fractions were obtained, by distillation under reduced pressure.

The PFPE surfactant and the PFPE oil used in this work have the same R_f group of general formula reported in the introduction.

The PFPE surfactant R_f–CF_2–$COO^- NH_4^+$, of narrow molecular weight distribution (95 % by gaschromatographic analysis), has a molecular weight of 710; R_f has $3 \div 4$ monomer units. After the neutralization of the PFPE acid (R_f–CF_2–COOH) with aqueous ammonia, the surfactant was dried at 60 °C under vacuum for several days. The water content of the surfactant, as determined by Karl Fisher titration in anhydrous methanol is 0.28 % by weight. From now on, the latter water content will affect the surfactant concentration values. The surfactant, which is highly hygroscopic, was stored under vacuum.

The PFPE oil R_f–CF_3 (narrow molecular weight distribution) has a molecular weight of 800, thus R_f has 4 monomer units. The oil is a transparent liquid of density 1.8 g/cm^3, index of refraction 1.282 and viscosity 0.0684 poises; its ability to solubilize air is 26 cm^3 of air every 100 cm^3 of oil; the solubility in water is 14 10^{-6} w/w.

Isopropyl alcohol of RPE grade (Carlo Erba, Italy) and double distilled or Millipore Milli-Q water have been used.

Methods

a) Surface and interfacial tension were determined at 25 °C by the Du Nouy ring method on a Kruss 110 tensiometer.

b) Differential scanning calorimetry (DSC). The study of the thermal properties of the PFPE surfactant was performed with DSC by means of a Mettler TA 3000 thermal analyzer equipped with a DSC-30 low temperature cell. The heat flow rate (dQ/dt) vs temperature was recorded at constant pressure during the controlled heating of previously frozen surfactant samples (DSC-ENDO). The temperature rate (dT/dt) of 4 °C/min was used in the DSC-ENDO measurements of samples frozen with a 2 °C/min scan speed. The temperature interval investigated extends from −130 ° to +100 °C.

c) Quasi-elastic light scattering analysis (QELS) was performed on a Brookhaven apparatus (BI – 200SM goniometer plus BI – 2030 AT correlator and computer with 128 channels) with a time resolution of 0.1 μs. The light source is a vertically polarized Argon ion laser (Spectra Physics series 2000, $\lambda = 514.5$ nm) steadily kept at 0.1 W power. A calibration procedure was carried out on a dilute monodispersed suspension of polystyrene latex spheres. The data were analyzed using the cumulant technique (software provided by Brookhaven Instrument Co.). The correlation function is expanded about an average linewidth $\bar{\Gamma}$ as a polynomial in the sample time with cumulants as parameters to be fitted [5, 6]. The expansion is stopped at the second moment result and a weighted, least-squares technique is applied to the second order polynomial to determine the constants and their standard deviations. The so-called average mutual diffusion coefficient $\bar{D}$ is related to $\bar{\Gamma}$ by the relation $\bar{D} = \bar{\Gamma}/K^2$ where $K = (4\pi/\lambda)\, n \sin(\theta/2)$ is the scattering wave vector, n the index of refraction of the sample and θ the scattering angle. The deviation of the experimental curve from a single exponential decay is usually given by $\mu_2/\bar{\Gamma}^2$ (where μ_2 is the second moment of the distribution) and called "degree of polydispersity" [6]. In some cases multi-exponential fittings were done by a non-negatively constrained least squares method (software provided by Brookhaven Instrument Co.). Dust-free samples were obtained by filtration through Millipore filters ($0.2 \div 0.45$ μm-pore size). For samples exhibiting high scattering power, where the scattering due to dust is relatively low with respect to the scattering of the sample itself, measurements were carried out before and after filtration, to test if a variation was induced on the sample by the filtration procedure. No significant difference in the measured variables was observed, thus the filtration procedure seems not to modify the samples.

d) Light Intensity Measurements. The intensity of the scattered beam has been measured as total counts of photon (accumulated during one experimental run) divided by the experimental duration in seconds over identical scattering volumes for all the samples. The statistical error is the standard deviation over several measurements. Angular intensity measurements on two Rayleigh scatterers (benzene and toluene) have been done in the range $45° \div 150$ °C; the measured values (corrected for dead time, dark count, and scattering volume effects) are identical, with a deviation between the values of less than 3 %.

Results and discussion

Surface and interfacial tension measurements

The surface tension of PFPE oil is 20 dynes/cm at $T = 25$ °C. The interfacial tension PFPE oil/water is 40 dynes/cm; the addition of PFPE surfactant decreases the interfacial tension to few dynes/cm. Furthermore, a critical micellar concentration C.M.C. = 3 10^{-5} mole/liter has been measured and the surface tension of $\simeq 15 \div 20$ dynes/cm has been found for the water – surfactant solution at concentrations higher than the C.M.C. value.

DSC Analysis

The DSC analysis was done on the PFPE surfactant. The thermal spectra (endotherms a–b and c) are reported in Fig. 1. The thermal curve (a) corresponds to the very first experimental run made; curves (b) and (c) are successive measurements on the same sample. The only remarkable difference consists in the disappearence of the thermal event at $T \sim 50$ °C in the DSC spectra (b) and (c). The latter behavior seems to be characteristic of the given surfactant as it results from visual observation of this component in the thermal range $20° \div 80$ °C. The surfactant is white and solid for $T < 40$ °C; its aspect changes gradually from white to transparent in the range $40° \leq T \leq 50$ °C but it remains solid in this range. At $T \simeq 50$ °C the surfactant becomes a transparent not birefringent fluid of very high viscosity; the viscosity decreases slowly for a temperature increase towards 80 °C. During following runs between 20 °C and 80 °C the surfactant remains transparent solid, or transparent liquid of high viscosity, depending on the temperature value. The heating

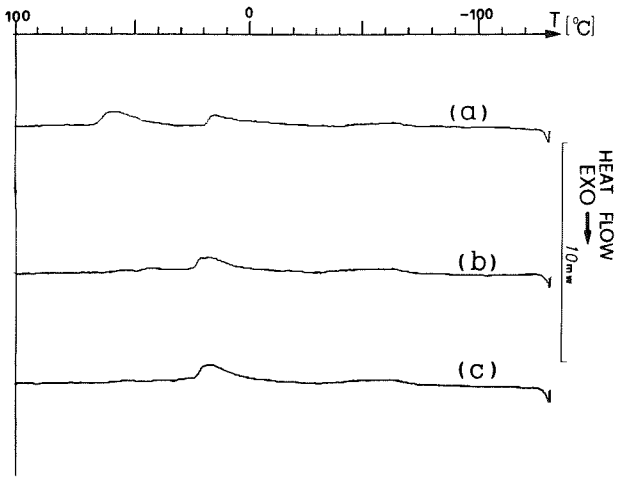

Fig. 1. DSC recordings of the PFPE surfactant: three successive measurements of the same sample are shown

at $T > 50\,°C$ seems to be necessary to obtain an homogeneous structure from the initial complex organization of the surfactant.

Phase diagram

For each binary, ternary, and quaternary phase diagrams of PFPE surfactant, PFPE oil, water, and isopropyl alcohol mixtures of given composition were prepared at room temperature and put into glass tubes (closed by teflon plugs). Each sample was stabilized at 80 °C in order to enhance the solubility before starting the phase diagram investigation. At the end of the stabilization time the number of phases was counted and the behavior of each phase described after examination by visual observation and between two crossed polarizers. Phase equilibrium was considered as achieved when no further change appeared with time. The stabilization time, which strongly depends on the composition and/or nature of the samples, was more than 5 h in the range 40° ÷ 60 °C and more than 10 h in the interval 20° ÷ 40 °C. The thermal range investigated is 20° ÷ 60 °C.

The following symbols and abbreviations have been used throughout: C is the concentration of one component over the total sample amount in w/w. For the phase diagrams: 1ϕ corresponds to monophasic, isotropic, homogeneous and transparent domains; 2ϕ corresponds to biphasic transparent domains. S: surfactant, O: oil, W: water and A: alcohol. If not otherwise specified, a 10 % composition step was used to prepare the samples for phase diagram investigation.

The binary phase diagrams of surfactant – water, surfactant – oil, and oil – water systems are reported in Fig. 2. The following informations can be deduced:

a) The surfactant – water system gives birefringent phases for any composition at any temperature tested;

b) Surfactant is insoluble in oil for $T < 30\,°C$ for any composition tested; the samples are transparent solid homogeneous not birefringent for an oil concentration $C < 30\,\%$, while for $C \geq 30\,\%$ two phases are observed, the lower is white – turbid and the upper is transparent – fluid (see Fig. 2, PP' line). For temperatures higher than 30 °C solubility is achieved. Surfactant – oil samples belonging to the monophasic domain are characterized by differences in the fluidity value; at a given temperature the fluidity increases gradually from the surfactant rich corner to the oil rich corner.

c) As shown in the experimental section, the water solubility in oil is too low to be reported in the phase diagram scale.

The surfactant – alcohol and the oil – alcohol systems have been also studied in the range 20 ° ÷ 60 °C. Isopropyl alcohol solubilizes surfactant at any concentration higher than 5 % and practically at any temperature tested. However it is insoluble in oil. We recall that isopropyl alcohol is soluble in water in any proportion.

The ternary phase diagram of the surfactant – oil – water system is reported in Fig. 3 where the monophasic domains at three main temperatures are shown. The monophasic domain (transparent not birefringent

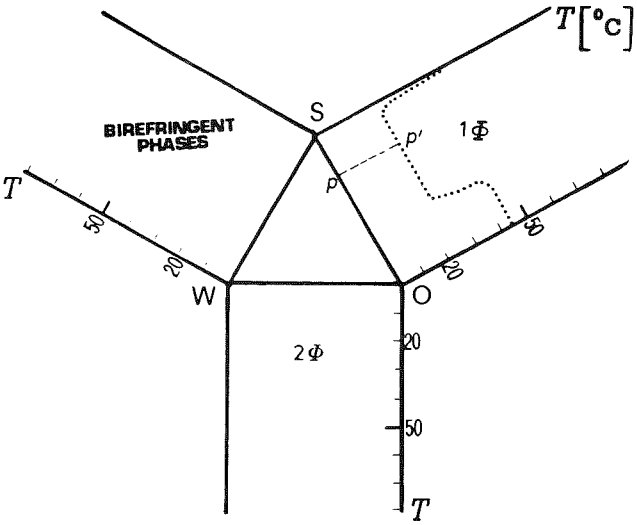

Fig. 2. Binary phase diagrams investigation of the S-W, W-O, and O-S mixtures

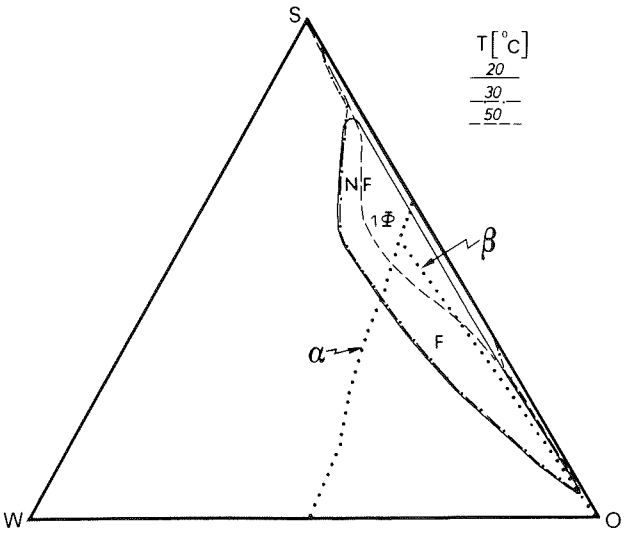

Fig. 3. Ternary phase diagram of the system S-W-O mixture. Monophasic regions are shown as a function of temperature. α- and β-lines identify excluded regions on the basis of geometrical considerations. *NF* and *F* symbols identify not-fluid samples, respectively

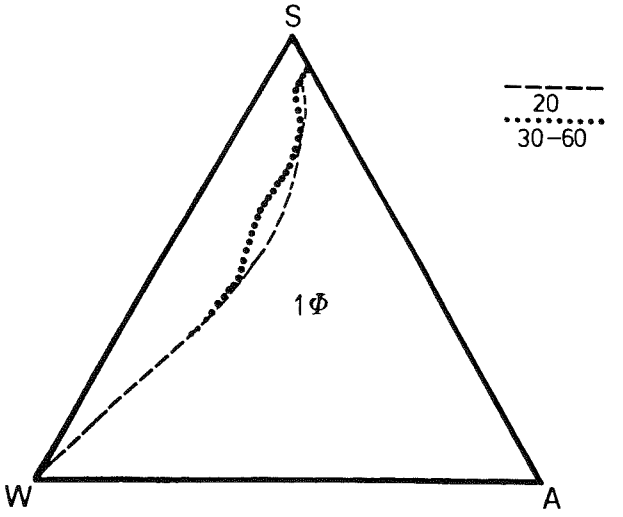

Fig. 4. Ternary phase diagram of the S-W-A mixture. Monophasic regions are shown as a function of temperature

samples) is close to the oil – surfactant side at all the temperatures in the range 20° ÷ 60 °C. At $T = 20$ °C the domain is a loop, along the S–O side; the maximum water amount of the domain is ~ 17 %. At $T =$ 30 °C the loop remains the same as before but it opens towards the O–S side in the range 5 ÷ 60 % of oil. At T = 50 °C the domain becomes thinner (the maximum water amount is 12 %) and wider along the O-S side. The sample viscosity tends to decrease upon approaching the oil rich corner. Therefore poorly fluid samples (*NF*) as well as fluid samples (*F*) are observed (see Fig. 3).

In Fig. 4 the ternary phase diagram of the surfactant – water – alcohol system is reported. The monophasic domain is very large for all the temperatures tested. The minimum alcohol amount which solubilizes any proportion of the surfactant – water mixture is about 20 %. This phase diagram shows the great ability of the alcohol to solubilize both surfactant and surfactant plus water birefringent phases suggesting that the alcohol may affect the interfacial film curvatures.

In Fig. 5 pseudoternary phase diagrams of the surfactant – alcohol – oil – water system are reported. The surfactant plus alcohol mixture is considered as a pseudocomponent. Four main S/(S + A) ratios were studied, namely: 0.6, 0.7, 0.8, and 0.9 (w/w). They correspond respectively to the molar ratios 0.13, 0.19, 0.34, and 0.76. The thermal range studied is always 20° ÷ 60 °C. For the lower ratio S/(S + A) = 0.6 the monophasic region is narrow, strictly close to the water side and independent of the temperature. At S/(S + A) = 0.7 the monophasic domain enlarges from the water side towards the oil corner to cover regions having oil content always lower than 20 %. At S/(S + A) = 0.8 the monophasic domain changes drastically; the solubility towards the water side is decreased; however the solubility towards the oil side is increased. The domain enlarges for temperature increase. At S/(S + A) = 0.9 the monophasic domain is very narrow and close to the oil side; a temperature increase, increases the solubility along the same side.

From the investigation of binary and ternary phase diagrams (Figs. 2 and 3), the following main considerations can be made:

a) At $T < 30$ °C the surfactant is insoluble in water as well as in oil; however the larger monophasic domain is exhibited by the W–S–O system.

b) At T > 30 °C, against a temperature increase, the surfactant becomes more and more soluble in oil and the monophasic domain correspondingly spreads towards the O–S side. The increase of the surfactant solubility in oil decreases the ability of the S–O mixture to solubilize water.

From the previous considerations we can deduce that, at T < 30 °C, some structural organization of the components water, surfactant, and oil could explain the formation of the wide monophasic domain. Furthermore, from composition considerations, only water in oil structures can be hypothesized for this domain. However, we cannot a priori exclude a simple

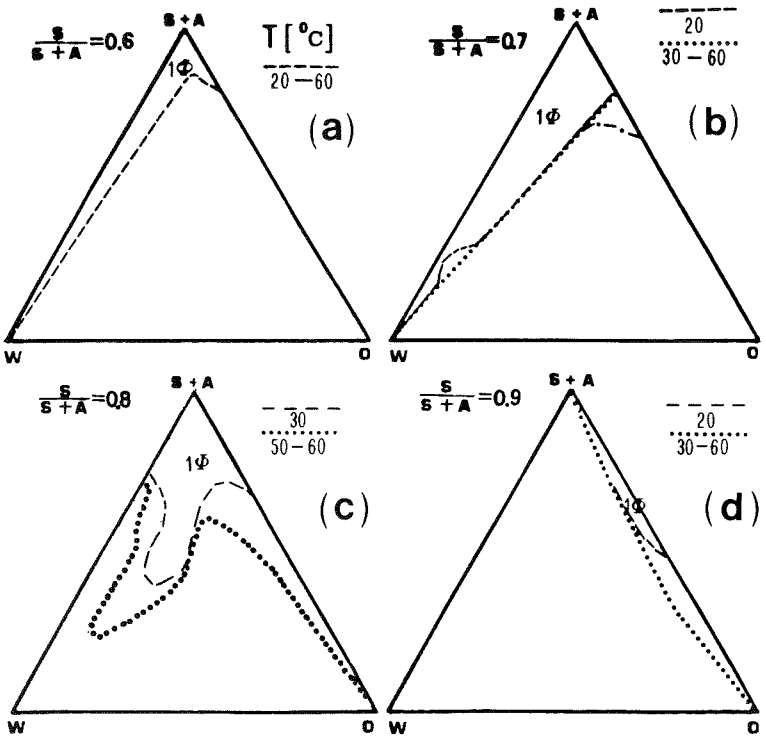

Fig. 5. Pseudoternary phase diagrams of the mixture S–A–W–O for different S/(S + A) ratios (% w/w). The temperature dependence of monophasic domain is also shown

cosolubilization of the components. In the case that water in oil droplets exist, it is reasonable to suppose the water inside the core and the surfactant at the interface while the oil is the continuous medium. From geometric considerations [7], two excluded regions for w/o structures should be taken into account, one due to the close-packing limit and the other due to the minimum surface-limit available for the polar-head area of the surfactant, which can be roughly assumed at around 50 Å^2, as deduced from surface pressure-area curves [8]. The close-packing limit of hard spheres, 0.64, can be expressed as: $\phi = (V_w + V_s)/(V_o + V_w + V_s)$ where V are the volumes of water, surfactant, and oil, respectively. In Fig. 3 the α line has been calculated for $\phi = 0.64$, assuming for the density of surfactant and oil the value 1.8 g/cm^3 because the two types of molecules are very similar (the excluded region falls in the upper part of the triangle). The polar-head area limit originates the β line which excludes the region very close to the S–O side. If σ is the surface polar-head area, R the droplet radius, l the surfactant length, V_s^* the surfactant molar volume, and N_A the Avogadro number, then:

$$\sigma = \left(\frac{3V_s^*}{N_A}\right)\left(\frac{(R-l)^2}{R^3-(R-l)^3}\right).$$

The last equation implies that under the hypothesis of constant l, the points of constant radius fall in the same locus as those of constant σ, the lower limit of σ being the area of the surfactant polar head. The l value of 13 Å is found from molecular weight and density values supposing a 50 Å^2 polar-head area. It is worth noting that the region identified through the geometrical evaluation agrees with the one found experimentally on the actual system for what concerns the low-viscosity domain (F) of isotropic fluid and transparent samples. We have to point out that the assumption that each component is insoluble in the others (which is fundamental for the geometrical model hypotheses) is very rough in our case, expecially because at oil concentrations less than 30%, the binary mixture S–O is an homogeneous transparent solid, at the visual observation, which induces us to think that some kind of interaction is possible between oil and surfactant. In order to detect whether structures exist in the monophasic domain of the S–W–O system, light-scattering investigations have been performed. As the index of refraction of the oil and of the surfactant tail must be approximatively the same, (because the two molecules have an identical R_f group), we expect a continuous medium charcterized by an index of refraction of 1.282 and a dispersed phase (water) of index of refraction 1.333.

Table 1. Sample composition in % w/w

	S1	S2	S3	S4	S5	S6	S7
S	47.80	9.54	45.93	28.24	18.65	41.78	9.44
O	49.98	90.01	44.06	64.78	74.13	51.37	88.98
W	2.25	0.45	10.01	6.98	7.22	1.97	0.45
A	–	–	–	–	–	4.88	1.14

The effect of the isopropyl alcohol addition to the ternary system S–O–W has been investigated specifically with the aim of finding water in oil structures. For ionic surfactants it is a general result that short chain alcohols are too soluble in the aqueous phase to be useful as cosurfactant [9]. For example, isopropanol is insoluble in sodium dodecyl sulfate and the monophasic domain of the ternary W–A–S occupies the region close to the W–A side. Since isopropanol solubilizes the PFPE surfactant quite well (see Fig. 4), we have carried out a preliminary investigation to test if isopropanol favors the formation of w/o, o/w structures or both, independently on the cosurfactant or cosolvent effect of the alcohol itself. From the phase diagram of Fig. 5 it is seen that the monophasic domain belongs either to the region accessible to w/o or to o/w structures; the above geometrical considerations can also apply to an o/w system [7]. It follows that light scattering investigation may offer some evidence for the presence of structures. Such a result would strongly support that a transition from w/o curvature to the o/w one, takes place due to the presence of the alcohol.

QELS and light intensity measurements

A preliminary QELS analysis has been carried out on ternary and quaternary systems with the aim of obtaining structural information [10, 11]. The composition of the samples investigated is reported in Table 1. For all the samples, the autocorrelation function of the scattered intensity has been measured at different angles in the angular range 45 °C ÷ 150 °C. Constant $\bar{\Gamma}/K^2$ values have been detected; therefore the scattering process is diffusive and the mutual diffusion coefficient can be espressed by $\bar{D} = \bar{\Gamma}/2K^2$ (homodyne detection). As an example of the angular dependence, the $\bar{D}(\theta)$ values for sample S_2 at $T = 35$ °C are reported in Table 2. For the evaluation of the scattering wave vectors of all the samples analyzed, the index of refraction used was that of the oil (1.282) because the samples are mainly composed of oil. In fact, all the n values estimated by the refractivity formula [12] were found to differ less than 1% from the n value of oil. In Table 3 the $\bar{D}$ values at $\theta = 90°$ are reported for all the samples investigated. Furthermore, in Table 3, $\mu^2/\bar{\Gamma}^2$ and the intensity values are also given. For all the samples the I values have been detected at $\theta = 90°$. No sharp peak has been observed in the $I(\theta)$ dependence; further investigation on the $I(\theta)$ dependence will be the object of a future work. The $\bar{D}$ and I values reported in Table 3 are averages over several measurements; the standard deviations are also given. All the samples have been studied in cylindrical cells of identical diameter (12 mm). For sample S_4, which has an intermediate scattering power value between S_1 and S_5, a cylindrical cell of 26 mm diameter has been also used to test if multiple scattering affects the measurements. As the $\bar{D}$ values are identical, within the experimental error, it is reasonable to deduce that multiple scattering does not affect the results.

The oil-sample alone was also studied; no autocorrelation function could be found in the limit of resolution of the apparatus, and the intensity was practically undetectable.

Because oil by itself does not scatter light, the oil-rich samples (S_2, S_4 and S_5) scatter light strongly, therefore, some structural organization must be inside the S_2, S_4 and S_5 samples due to the presence of water and surfactant. In fact, the I values of S_2 S_4, and S_5 samples are the highest values detected (see Table 3). Correspondingly, $\bar{D}$ values in the range $1 \div 0.37 \times 10^{-8}$ cm^2/s have been obtained. In the frame of ternary samples, the S_1 and S_3 ones with about a 50% oil to surfactant ratio and a scattering power less than the S_2,

Table 2. Angular dependence of the mutual diffusion coefficient for S2 at $T = 35$ °C

θ	45°	60°	90°	120°	135°	150°
$\bar{D}(\theta) \times 10^8$ cm^2/s	1.23 ± 0.08	1.11 ± 0.09	1.19 ± 0.08	1.24 ± 0.06	1.22 ± 0.03	1.20 ± 0.03

Table 3. Light-scattering data

	S1	S2	S3	S4	S5	S6	S7
T(°C)	25	35	25	25	25	25	–
$\bar{D}(\theta) \times 10^7$ cm^2/s	0.84 ± 0.01	1.19 ± 0.08	0.86 ± 0.02	0.57 ± 0.01	0.37 ± 0.01	1.19 ± 0.02	–
$\mu_2/\bar{\Gamma}^2$	0.09	0.11	0.08	0.05	0.09	0.08	–
I(a.u.)	8.70 ±0.1	120 ± 1	17.6 ± 0.1	45.3 ± 0.1	149 ± 1.2	12.4 ± 0.1	–
T(°C)	50	50	–	25	–	50	50
$\bar{D}(\theta)10^7$ cm^2/s	2.14 ± 0.16	0.42 ± 0.02	–	0.58[a]) ± 0.02	–	2.82 ± 0.12	1.08 ± 0.02
$\mu_2/\bar{\Gamma}^2$	0.20	0.13	–	–	–	0.13	0.04
I(a.u.)	8.20 ± 0.05	85.9 ± 1.4	–	–	–	10.6 ± 0.1	41.4 ± 0.7

[a]) cell diameter 26 mm

S_4, and S_5 samples, a $\bar{D}$ value falls within the previous range.

In summary, all the ternary samples of Table 3 appear to possess a structural organization. As the water content of all the samples is lower than 10 % we can hypothesize that the samples are of water-in-oil-type; a simple cosolubilization of the components can therefore be excluded. The degree of polydispersity, always lower than 10 % at $T = 25$ °C and lower than 20 % at all the temperatures tested, may support the interpretation that the samples are practically monodispersed. In fact, even for the highest $\mu_2/\bar{\Gamma}^2$ value (20 %), a single-peak distribution was obtained by the NNLS technique.

Light-scattering measurements were also done on samples of the monophasic regions of the phase diagrams b, c, and d of Fig. 5. For the phase diagrams b and c (samples close to the W–(S + A) side), the autocorrelation functions display multiexponential decays and the intensity values are lower than those of samples of Table 3. However, a structural organization is exhibited as QELS signals have been detected. A quantitative investigation will be carried out in future work. On the basis of considerations about the relative proportions between the components, it is reasonable to expect o/w structures. For the phase diagram d of Fig. 5 two samples have been investigated (S_6 and S_7 of Table 1). $\bar{D}$, I and $\mu_2/\bar{\Gamma}^2$ values comparable with those of the ternary samples studied have been obtained. On the basis of geometric considerations, w/o structures are expected in the latter case.

All the samples have been studied at 25 °C if monophasic and transparent at that temperature; in case of phase separation as in the S_2 and S_7 samples, a study has been carried out a $T = 50$ °C. For comparison few other samples (S_1 and S_6) have also been studied at $T =$ 50 °C. In S_1 and S_6 samples $\bar{D}$ increases with temperature while in S_2 it decreases.

Conclusion

The hypothesis that microemulsions form by mixing, in given proportions, PFPE surfactant, PFPE oil and water (in presence or absence of isopropyl alcohol) is strongly supported by the phase diagram and light-scattering results. Typical samples (isotropic, transparent, and homogeneous) belonging to the monophasic regions of ternary and quaternary phase diagrams exhibit a structural organization. At the present state of the research, quantitative considerations about the dimensions of the structures, their geometry, as well as the interactions between the structural aggregates cannot be made. However some preliminary considerations can be put forward by comparing the findings of the studied samples which belong to the ternary phase diagram. For such samples, aggregates of water – surfactant type can be hypothesized as previously discussed. Furthermore, as the $\bar{D}$ value of the samples S_3, S_4, and S_5 decreases towards the oil-rich corner and the fluidity of the samples increases towards the same corner, we can reasonably think that the interactions between the aggregates are quite low in the S_5 sample. Thus we can give a rough estimate of the hydrodynamic radius R_H of the aggregates, assuming the $\bar{D}$ value close to the mutual diffusion coefficient at zero concentration of the dispersed phase. Using the Stokes-Einstein formula [10] and also assuming for the viscosity of the continuous medium that of the oil, an R_H value of 86 Å can be estimated, a value which is typical of microemulsion systems.

References

1. Chittofrati A, Lenti D, Sanguineti A, Visca M, Gambi CMC, Senatra D, Zhou Z, in press, Colloids & Surfaces, X Chemistry of Interfaces Conference, S Benedetto del Tronto, May 1988
2. Ceschin C, Roques J, Malet-Marrins MC, Lattes A (1985) J Chem Tech Biotechnol 35A:78
3. Selve C, Castro B, Lempoel P, Mathis G, Gartiser T, Delpuech JJ (1983) Tetrahedron 39:131
4. Sianesi D, Pasetti A, Fontanelli R, Bernardi GC, Caporiccio G (1973) Chim Ind 55:208
5. Koppel DE (1972) J Chem Phys 57(11):4814
6. Brown JC, Pusey PN, Dietz R (1975) J Chem Phys 62(3):1136
7. Biais J, Bothorel P, Clin B, Lalanne P (1981) J Colloid Interface Sci 80(1):136
8. Caporiccio G, Burzio F, Carniselli G, Biancardi V (1984) J Colloid Interface Sci 98(1):202
9. Friberg SE (1985) J Dispersion Sci and Technology 6(3):317
10. Guest D, Langevin D (1986) J Colloid Interface Sci 112:209
11. Chang NJ, Kaler EW (1986) Langmuir 2:184
12. Born M, Wolf E (1983) In: Principles of Optics. Pergamon Press

Received October, 1988;
accepted April, 1989

Authors' address:

C.M.C. Gambi
Dipartimento di Fisica
L.E. Fermi 2
I-50125 Florence, Italy